

# Nanoscale field emission structures for ultra-low voltage operation at atmospheric pressure

A. A. G. Driskill-Smith,<sup>a)</sup> D. G. Hasko, and H. Ahmed

*Microelectronics Research Centre, Cavendish Laboratory, University of Cambridge, Cambridge CB3 0HE, United Kingdom*

(Received 20 August 1997; accepted for publication 23 September 1997)

Novel field emission devices with electron path lengths an order of magnitude less than the elastic mean free path of electrons in air have been fabricated and tested at atmospheric pressure. The nanoscale-tip field emission system consisted of multiple emitter tips of radii about 1 nm within an extractor aperture of diameter 50 nm. The extractor turn-on voltage was approximately 7.5 V; field-emitted currents of up to 10 nA were collected at extractor voltages of less than 10 V. Maximum current densities of over  $10^{11}$  A m<sup>-2</sup> have been observed, and the emission stability in air at atmospheric pressure is better than 3%. © 1997 American Institute of Physics. [S0003-6951(97)01047-4]

Recent work on the miniaturization of microfabricated field emission (FE) devices for vacuum microelectronics has concentrated on the reduction of the radius of the emitter tip and the diameter of the extractor electrode aperture. Both these factors are known to reduce the extractor voltages required for field emission.<sup>1</sup>

Conventionally microfabricated FE devices, whether they consist of metal Spindt tips<sup>2</sup> or silicon tips,<sup>3,4</sup> operate in high vacuum; for only at pressures below  $10^{-6}$  mbar is the damage from ion bombardment to the emitter surface sufficiently low. To relax this requirement and enable a FE device to operate successfully at atmospheric pressure, two conditions must be satisfied: the dimensions of the device must be much less than the elastic mean free path of electrons in air (about 200 nm at low electron energies),<sup>5</sup> and the operating voltage must be less than the first ionization potential of molecules present in air (12.7 and 15.6 eV for nitrogen and water, respectively).<sup>6</sup> In this letter, we describe the fabrication and operating characteristics of a nanoscale FE device in which the electron path length is an order of magnitude less than the elastic mean free path of an electron in air. The device structure, consisting of multiple emitter tips of radii about 1 nm within an extractor electrode aperture of diameter 50 nm, is sufficiently compact to yield both an ultra-low turn-on voltage of about 7.5 V and operation at atmospheric pressure.

To form nanopillars with tip radii of about 1 nm we employed a granular metal mask. AuPd was deposited on a tungsten metal substrate to a nominal thickness of 1 nm by an ionized-beam deposition method.<sup>7,8</sup> This resulted in the nucleation of small AuPd grains of diameter  $2.5 \pm 0.5$  nm on the substrate. The AuPd grains acted as a self-aligned mask for an anisotropic reactive ion etch (RIE) process in which nanopillars whose tip radii were defined by the AuPd grain size were formed. The conditions for the RIE process were: 40 sccm CF<sub>4</sub> and 4 sccm O<sub>2</sub> gas mixture; 20 mTorr chamber pressure; 200 W rf power. An etch time of 15 s, corresponding to an etch depth of 10 nm in tungsten, was found to produce an appropriate combination of aspect ratio and sur-

face coverage of the nanopillars when the etch was performed over a large flat area of tungsten. The nanopillars that began to form under the smaller AuPd grains collapsed as the grains were undercut because the RIE process was not entirely anisotropic. The nanopillars that formed under the larger AuPd grains withstood the etch and had tip radii of about 1 nm and pillar heights of up to 10 nm. For an etch time greater than 20 s, all AuPd grains were completely undercut and all nanopillars were destroyed, while for an etch time less than 10 s, the surface coverage of nanopillars was so high that, on subsequent application of an electric field to the surface, the field enhancement at the nanopillar tips was insufficient to draw a field-emitted current. We assume that this was due to the shielding effect of nearby nanopillars.

The FE device fabrication process sequence is illustrated in Fig. 1. Initially the cathode metal (tungsten), dielectric (silicon dioxide), and extractor metal (tungsten) layers were rf sputtered onto a semiconductor substrate, and a 50-nm-diam extractor electrode aperture was defined by high-resolution electron beam lithography. To form the nanopillars, AuPd grains were deposited on the cathode metal inside the hole and subjected to a 15 s CF<sub>4</sub>/O<sub>2</sub> RIE process. Although over 100 grains were deposited in each 50-nm-diam device hole, there were only about 10–20 possible emission sites in each device. Most nanopillars collapsed during the etch process and only those that survived and were located near the center of the hole, where the etch rate was fastest, had sufficient aspect ratio to be useful emitters.

In our FE device structure the applied extractor voltage was limited by the breakdown voltage of the 30-nm-thick rf-sputtered SiO<sub>2</sub> used as the dielectric. This was 15 V in the case of a continuous film of 30-nm-thick SiO<sub>2</sub> (Fig. 2, curve D). For 30-nm-thick SiO<sub>2</sub> after fabrication of a FE device hole, but without nanopillars present within the hole, the breakdown voltage was typically reduced by 1 V. This was found both when no AuPd had been deposited within the hole and when AuPd had been deposited but had not been subjected to a RIE process (Fig. 2, curve C). The leakage current in the case of the FE device arose from surface conduction along the inside of the hole, but remained less than 2 nA up to an applied voltage of over 13 V. In the case of a

<sup>a)</sup>Electronic mail: aagd100@cus.cam.ac.uk

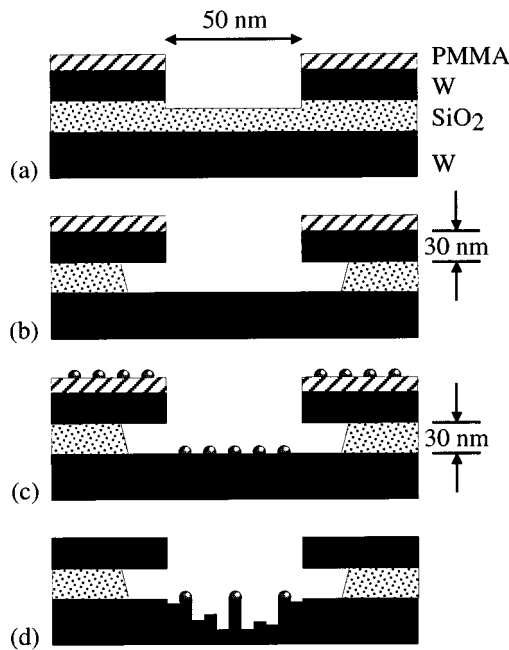


FIG. 1. Fabrication process sequence: (a) exposure and development of 50 nm disk in PMMA resist, and anisotropic RIE; (b) isotropic BHF etch; (c) deposition of AuPd grains; (d) RIE to form nanopillars, and resist strip. The AuPd grains and nanopillars are not to scale.

continuous film of SiO<sub>2</sub> the leakage current was less than 200 pA up to an applied voltage of 15 V.

The FE devices with nanopillars present within the device hole were tested in air at atmospheric pressure. Field-emitted electrons travelled ballistically from the nanopillar tips to the extractor electrode and were registered at atmospheric pressure as an extractor current. A typical extractor current–voltage ( $I$ – $V$ ) device characteristic is shown in Fig. 2, curve A. At forward bias, the FE turn-on voltage was 7.5 V. Several peaks were observed in the characteristic, at 9.8, 10.7, 11.8, and 12.3 V, before the current increased inexorably towards device breakdown between 13 and 14 V. At reverse bias the current registered was due solely to leakage

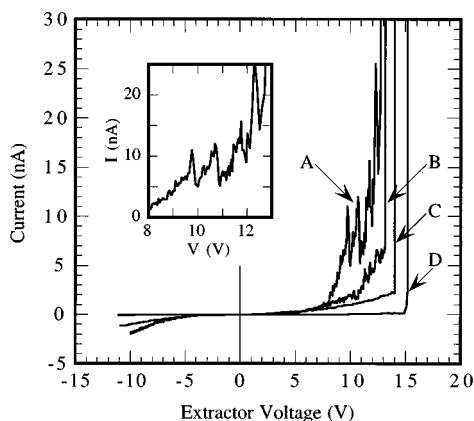


FIG. 2.  $I$ – $V$  characteristics for: A—a typical FE device with dielectric area 40  $\mu\text{m}^2$  and nanopillars present; B—a subsequent test of the same FE device; C—an equivalent device but without nanopillars; D—breakdown of a continuous film of 30-nm-thick SiO<sub>2</sub> of equivalent area. Inset: curve A expanded in the range 8–13 V.

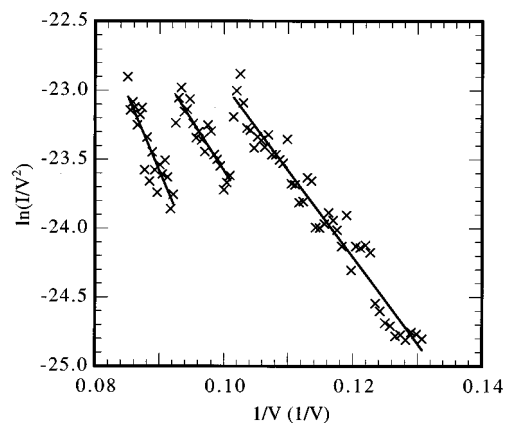


FIG. 3. Fowler–Nordheim plot for the device of Fig. 2, curve A. The three distinct ranges of data correspond to the first three peaks of Fig. 2, curve A.

through the dielectric and along the inside of the device hole. Very similar results were obtained when the FE devices were tested in ultrahigh vacuum at pressures below  $10^{-8}$  mbar.

No field-emitted electrons were detected when nanopillars were not present within the device hole, i.e., when no AuPd had been deposited and the cathode metal surface was flat, or when AuPd had been deposited but not been subjected to a RIE process. The device characteristic in these cases was identical to that of Fig. 2, curve C.

The current that was detected above 7.5 V when and only when nanopillars were present was due mainly to emission from the nanopillar tips, where the geometrical field enhancement caused the local electric field to exceed the critical value of  $10^9$  V m<sup>-1</sup> required for field emission. Owing to the exponential dependence of field-emitted current on extractor voltage it is probable that, at any particular extractor voltage, the one tip with the greatest local electric field was the dominant source of field-emitted electrons. This tip is likely to have been the one with the largest aspect ratio and the least shielding from surrounding nanopillars. We therefore believe that the sudden fall in current at each of the peaks in the characteristic of Fig. 2, curve A, resulted from the destruction of the dominant nanopillar source of electrons at that particular voltage, followed by the activation of the next most prominent nanopillar. This view was supported by a subsequent test of the same device. The extractor current remained less than 2.5 nA up to an extractor voltage of 11 V, implying that the more prominent emission sites which had turned on below this voltage in the previous test had indeed been destroyed (Fig. 2, curve B).

Figure 3 shows the Fowler–Nordheim plot associated with the  $I$ – $V$  characteristic of Fig. 2, curve A, in the region 7.5–11.8 V. There are three distinct ranges of data, which correspond to the data near the first three peaks of the  $I$ – $V$  characteristic. A separate straight line may be fitted to each of the data ranges, confirming that each of the peaks arose from a FE process. From the gradient and intercept of the straight line corresponding to the first peak, a voltage conversion factor  $\beta$  of  $2.2 \times 10^8$  m<sup>-1</sup> and an apparent emission area  $\alpha$  of  $(0.19 \text{ nm})^2$  can be calculated,<sup>5</sup> where  $E = \beta V$ ,  $I = \alpha J$ ,  $E$  is the electric field at the emitter tip,  $V$  is the extractor voltage,  $I$  is the emission current, and  $J$  is the emis-

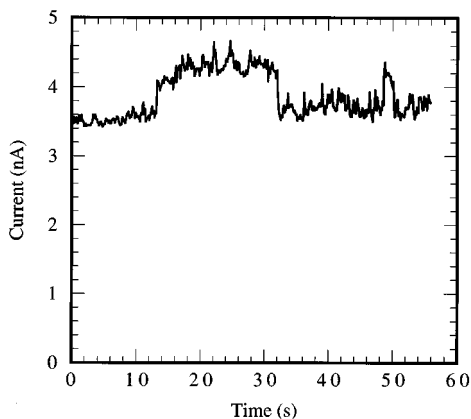


FIG. 4. Emission stability of a typical FE device.

sion current density. We also assume a work function at the emitter tip of 4.5 eV. The calculated voltage conversion factor  $\beta$  is equivalent to a geometrical field enhancement factor<sup>9</sup>  $\gamma$  of approximately 6.6. From the value of the FE current at the peak and the calculated apparent emission area  $\alpha$ , a maximum FE current density  $J$  of  $3 \times 10^{11} \text{ A m}^{-2}$  prior to breakdown of the first nanopillar source is calculated. This compares with the current density in FE systems of about  $10^{12} \text{ A m}^{-2}$  at which thermal destruction of the cathode is known to occur.<sup>1,10,11</sup> The straight line corresponding to the second peak yields  $\beta = 1.9 \times 10^8 \text{ m}^{-1}$ ,  $\alpha = (0.27 \text{ nm})^2$ ,  $\gamma = 5.6$ ,  $J = 2 \times 10^{11} \text{ A m}^{-2}$ . These results indicate that the emission area in both cases was of atomic size and that the second nanopillar source had both a larger emission area and a smaller aspect ratio than the first. In addition, the maximum current density immediately before destruction of the second nanopillar was virtually equal to that of the first, which suggests that there was a limiting emission current density common to all nanopillars at which they were destroyed.

We also measured the stability of the FE system in air at atmospheric pressure (Fig. 4). The emission current, while stable to within 3% for periods of tens of seconds, made occasional discrete jumps to other values. Such an effect, which has been observed in other FE systems, is believed to be due either to an atom being adsorbed or desorbed from the emitter tip, or to a “flip-flop” pseudoperiodic motion of an atom on the tip between two or more metastable positions.<sup>12,13</sup>

In conclusion, we developed and tested a nanoscale-tip field emission system with an electron path length much less than the electron mean free path in air, consisting of multiple field emission tips of radii about 1 nm within an extractor electrode of diameter 50 nm. The turn-on voltage was 7.5 V and the system operated stably in air at atmospheric pressure. The  $I$ – $V$  characteristic of any particular FE device was both repeatable and reproducible, provided the applied extractor voltage did not exceed about 10 V. We believe therefore that these devices may be useful in the future, although they still need to be characterized more fully to confirm this.

<sup>1</sup>T. Utsumi, IEEE Trans. Electron Devices **38**, 2276 (1991).

<sup>2</sup>C. A. Spindt, I. Brodie, L. Humphrey, and E. R. Westerberg, J. Appl. Phys. **47**, 5248 (1976).

<sup>3</sup>Y. Yamaoka, T. Goto, M. Nakao, S. Kanemaru, and J. Itoh, Jpn. J. Appl. Phys., Part 1 **34**, 6932 (1995).

<sup>4</sup>W. Mehr, A. Wolff, H. Frankenfeld, T. Skaloud, W. Höppner, E. Bugiel, J. Lärz, and B. Hunger, Microelectron. Eng. **30**, 395 (1996).

<sup>5</sup>T. K. S. Wong and S. G. Ingram, J. Phys. D **26**, 979 (1993).

<sup>6</sup>V. I. Makhov, Inst. Phys. Conf. Ser. **99**, 235 (1989).

<sup>7</sup>W. Chen and H. Ahmed, J. Vac. Sci. Technol. B **11**, 2519 (1993).

<sup>8</sup>W. Chen, H. Ahmed, and K. Nakazato, Appl. Phys. Lett. **66**, 3383 (1995).

<sup>9</sup>A. C. F. Hoole, D. F. Moore, and A. N. Broers, J. Vac. Sci. Technol. B **11**, 2574 (1993).

<sup>10</sup>P. R. Schwoebel and I. Brodie, J. Vac. Sci. Technol. B **13**, 1391 (1995).

<sup>11</sup>R. Gomer, *Field Emission and Field Ionization* (Harvard University, Cambridge, MA, 1961).

<sup>12</sup>C. Py and R. Baptist, J. Vac. Sci. Technol. B **12**, 685 (1994).

<sup>13</sup>M. Nagao, M. Matsubara, K. Inoue, Y. Gotoh, H. Tsuji, and J. Ishikawa, Jpn. J. Appl. Phys., Part 1 **35**, 5479 (1996).